Computers in Biology and Medicine 93 (2018) 149–157

Contents lists available at ScienceDirect

Computers in Biology and Medicine

journal homepage: www.elsevier.com/locate/compbiomed

Mechanistic modelling of drug release from multi-layer capsules

Badr Kaoui [a,b], Marco Lauricella [c], Giuseppe Pontrelli [c,*]

[a] Biomechanics and Bioengineering Laboratory (UMR 7338), CNRS, Sorbonne Universités, Université de Technologie de Compiègne, 60200 Compiègne, France
[b] Labex MS2T "Control of Technological Systems-of-Systems", CNRS, Sorbonne Universités, Université de Technologie de Compiègne, 60200 Compiègne, France
[c] Istituto per le Applicazioni del Calcolo - CNR, Via dei Taurini 19, 00185 Rome, Italy

ARTICLE INFO

Keywords:
Drug release
Multi-layer capsules
Pharmacokinetics
Diffusion equations

ABSTRACT

We propose a novel *in silico* model for computing drug release from multi-layer capsules. The diffusion problem in such heterogeneous layer-by-layer composite medium is described by a system of coupled partial differential equations, which we solve analytically using separation of variables. In addition to the conventional partitioning and mass transfer interlayer conditions, we consider a surface finite mass transfer resistance, which corresponds to the case of a coated capsule. The drug concentration in the core and through all the layers, as well as in the external release medium, is given in terms of a Fourier series that we compute numerically to describe and characterize the drug release mechanism.

1. Introduction

Nowadays, there is a tremendous increasing interest in using capsules as targeted drug delivery systems [1]. They allow enhanced therapeutic efficacy and reduce side effects by controlling the drug dose released in the human body. Capsules consist usually of a drug-loaded (fluid or solid) core surrounded by one or few hydrogel layers. Such encapsulation with multiple layers enhances the capsule mechanical stability, its biocompatibility, protects the active ingredients from external chemical aggression and premature degradation, and extends the sustainability of the drug release [2,3]. Different technologies have emerged in the last years to design and build layer-by-layer concentric spherical capsules [4–6], even though the release of their encapsulated drug cannot be fully predetermined. For some specific applications, a thin coating shell (or membrane) is required to envelop the whole structure in order to protect it from external chemical aggressions and mechanical erosion. Depending on the nature of the encapsulated formulations and according to the final aimed therapeutic requirements the typical size of these drug carriers can range from some nano- to milli-meters. For biomedical applications, micro-capsules are largely used [7–9].

Drug release characterization consists in tracking the kinetics of the drug eluted from the capsule into the external targeted medium, which is away from being an easy task in both cases *in vitro* and *in vivo*. However, effort and costs of developing and designing new optimized delivery devices can be dramatically reduced if the release mechanism is understood in advance using appropriate *in silico* models [10–12]. A number of review papers have summarized previously proposed models for drug release either from coated formulations [13–15] or from polymeric matrices [11,16]. There are also works on drug release from capsules [3,17–19], most of them dealing with empirical models. Here, we are rather interested in mechanistic models, because they allow a better understanding of the underlying mechanism of the drug release by tracking the influence of each physical input parameter, in contrast with the empirical models. We upgrade existing mechanistic models by extending their applications to the multi-layer coated capsules. Thus, predictable simulations based on those models can spot the significant physical parameters and allow extracting reliable information for conducting *in vitro* and *in vivo* experiments. Diffusion is by far the dominant mechanism in drug delivery beside other physico-chemical factors, such as osmosis, drug dissolution, and polymer swelling [13]. Most of the previous proposed mathematical models for release from spheres, as well as dissolved or dispersed drug systems, rely on oversimplifying assumptions, such as considering a constant diffusion rate and a well stirred (or at constant concentration) release medium [20], as summarized in the review by Arifin et al. [21]. As a matter of fact, the release characteristics strictly depend on the medium properties and these cannot be superficially dismissed or lumped in terms of boundary conditions at the capsule's surface as made elsewhere. Mass flux resistance at the coating surface is not properly addressed in literature.

In this article, we will make a step forward by studying theoretically for the first time the drug release from a multi-layer capsule, via a semi-analytic procedure, and moreover by avoiding considering simplistic

* Corresponding author.
E-mail address: giuseppe.pontrelli@gmail.com (G. Pontrelli).

https://doi.org/10.1016/j.compbiomed.2017.12.010
Received 17 October 2017; Received in revised form 11 December 2017; Accepted 14 December 2017

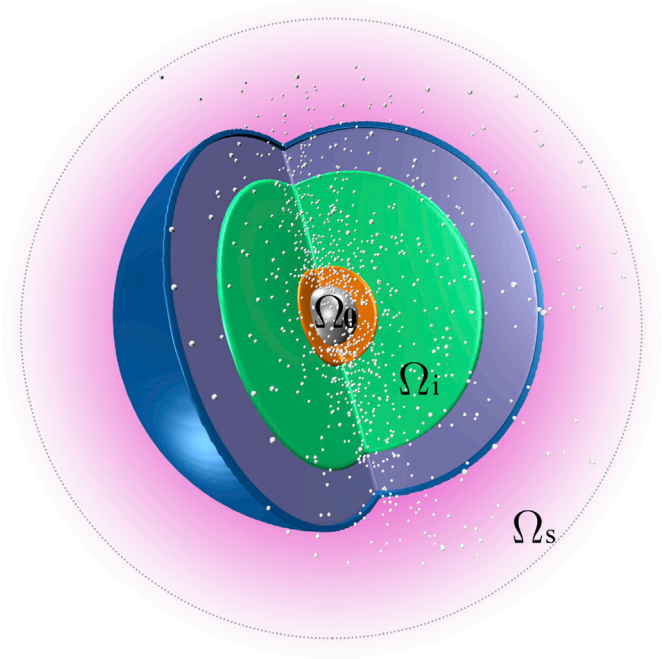

Fig. 1. Drug releasing from a multi-layer microcapsule. Drug is initially loaded in the core Ω_0 and diffuses, through all the intermediate layers Ω_i, into the release medium Ω_s confined by the dotted line. Suitable conditions are set at internal interlayer interfaces and at the external coating shell (figure not to scale).

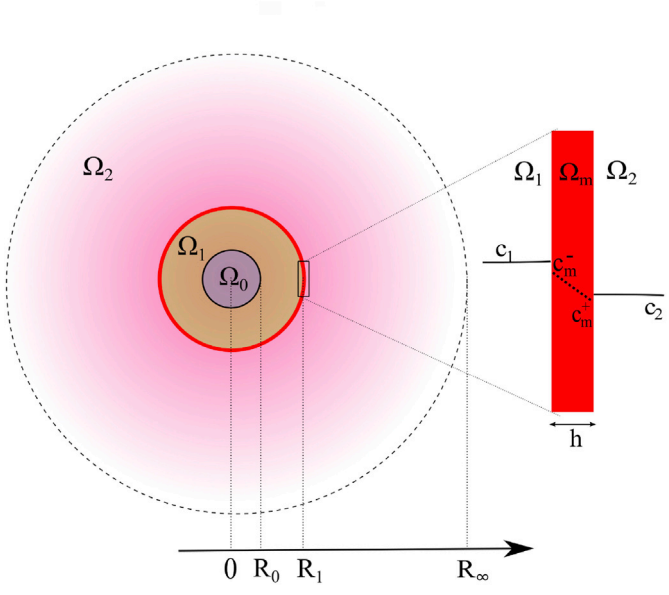

Fig. 2. Schematic representation of the cross-section of the radially symmetric multi-layer capsule, made of a central core Ω_0, a concentric shell Ω_1 and a thin protecting coating Ω_m (in red). Together with the external release medium Ω_2 - limited by the dashed line - it constitutes a three concentric layers system. On the right side, a zoom of the distributed coating layer shell (figure not to scale). (For interpretation of the references to colour in this figure legend, the reader is referred to the Web version of this article.)

hypothesis made elsewhere previously, such as a continuous concentration across the capsule surface. Following a preliminary work [22], we give a general presentation of a pure diffusive model through a composed layer-by-layer medium in Sect. 2. The specific case of a spherical core-layer capsule coated with a protective thin shell is addressed in Sect. 3, with a mathematical treatment somehow similar to the one we previously used for other drug-eluting systems [23,24]. Here we describe in detail this method and how to use it for the problem at hand. Special care is taken when setting the interlayer conditions, including the finite resistance (jump in the concentration value) at the external coated shell. An analytic expression for the concentration and the cumulative mass in all layers are given in Sect. 4. Finally numerical simulations are used to show concentration and mass profile in some configuration and study the dependence and sensitivity of the system to parameters.

2. A general model for drug release from a multi-layer capsule

Let us consider a multi-layer capsule made of a drug-filled core (the depot, Ω_0) surrounded by a number of layers (Ω_i, with $i = 1, 2, \ldots, n$) as illustrated in Fig. 1. These enveloping layers are constituted of different, but homogeneous and isotropic materials, which are customized to allow selective diffusion, to better control the release rate and sometimes to host more than one drug [7]. The last protective outer shell is in contact with the targeted release medium Ω_s (either a bulk fluid or tissue), here of finite extent, but with boundaries "*far enough*" from the capsule surface. Even in such a simple configuration where the transport is driven by pure diffusion, predicting drug kinetics is not an easy task.

In the core Ω_0, we assume that the drug dissolution occurs in a short time compared to that of diffusion and thus, can be considered as instantaneous [25]. Therefore, the drug diffusion in Ω_0 can be described by the second Fick's law:

$$\frac{\partial c_0}{\partial t} = D_0 \nabla^2 c_0 \text{ in } \Omega_0, \tag{2.1}$$

where c_0 is the concentration field and D_0 is the diffusion coefficient of the drug in the core. Analogously, in the surrounding layers and in the release medium Ω_s, we have similar diffusion equations

$$\frac{\partial c_i}{\partial t} = D_i \nabla^2 c_i \quad \text{in } \Omega_i \quad i = 1, 2, \ldots, n, s \tag{2.2}$$

with D_i is the diffusion coefficient in the i-th layer Ω_i (any possible convection, as in Ref. [26] or reaction terms in Ω_s are excluded). We set a perfect sink condition far away (see Sect. 3):

$$c_s = 0 \text{ at } \partial\Omega_s, \quad t > 0 \tag{2.3}$$

The initial condition for concentrations:

$$c_i(\cdot, 0) = f_i(\cdot) \quad \text{in } \Omega_i \quad i = 0, 1, \ldots, n, s \tag{2.4}$$

are given in all layers.

Here, we refrain from using two widely exploited over-simplistic assumptions [20,21], i.e.:

i) c_0 is constant at core surface $\partial\Omega_0$, as if there is a sustained source of drug;
ii) c_s is uniform in the release medium Ω_s, as in well-stirred medium.

2.1. Modelling interlayer boundary conditions

At each interface between two adjacent layers, flux continuity holds:

$$-D_i \nabla c_i \cdot \boldsymbol{n} = -D_{i+1} \nabla c_{i+1} \cdot \boldsymbol{n} \quad \text{at } \partial\Omega_i \cap \partial\Omega_{i+1} \tag{2.5}$$

with $\boldsymbol{n}$ the surface external normal vector. Moreover, a non-perfect contact due to the drug partitioning is present at the interlayers [27]:

$$c_i = \sigma_i c_{i+1}, \quad \text{at } \partial\Omega_i \cap \partial\Omega_{i+1} \tag{2.6}$$

where σ_i is the drug partition coefficient between layers i and $i+1$.

2.2. Modelling the external coating shell

To prevent fast delivery, the capsule's outmost layer Ω_n is protected

with a thin semi-permeable shell (*coating*) Ω_m having a small, yet finite thickness (h) (see Fig. 2 for the case $n = 1$). This coating shields and preserves the encapsulated drug from degradation and fluid convection, protects the inner structure, and guarantees a more controlled and sustained release [17]. Instead of using a distributed model as above, we model the drug diffusion across Ω_m by setting a simple interface boundary condition between Ω_n and Ω_s that incorporates the physical properties of the coating shell as follows. The mass flux across Ω_m is proportional to the concentration gradient:

$$\boldsymbol{J}_m = -D_m \nabla c_m \tag{2.7}$$

where D_m is the diffusion coefficient in the coating shell. Let σ_n and σ_m be the partition coefficients (i.e. the ratio of the inner/outer concentrations at the equilibrium, see Fig. 2 for the case $n = 1$) of drug on both interfacial sides of the coating shell:

$$\sigma_n = \frac{c_n}{c_m^-}, \quad \sigma_m = \frac{c_m^+}{c_s} \tag{2.8}$$

By applying Eq. (2.7) across the coating shell thickness h (Fig. 2, right zoom), we get:

$$\boldsymbol{J}_m \cdot \boldsymbol{n} = -D_m \frac{c_m^+ - c_m^-}{h} = \frac{D_m}{h}\left(\frac{c_n}{\sigma_n} - \sigma_m c_s\right) = \frac{D_m}{h\sigma_n}(c_n - \sigma_n \sigma_m c_s) \tag{2.9}$$

This can be viewed as an additional boundary condition, of different nature, imposed at the interface separating Ω_n and Ω_s. Thus, in case of having coating shell, Eqns (2.5)–(2.6) are then replaced with:

$$-D_n \nabla c_n \cdot \boldsymbol{n} = -D_s \nabla c_s \cdot \boldsymbol{n} = P(c_n - \Sigma c_s) \quad \text{at } \partial\Omega_n \cap \partial\Omega_s \tag{2.10}$$

where $P = \frac{D_m}{h\sigma_n}$ is the surface mass transfer coefficient (ms^{-1}) expressing the coating finite resistance and $\Sigma = \sigma_n \sigma_m$.

Equation (2.10) lumps the distributed model in Ω_m into a simpler interlayer boundary condition, where P reflects the shell mass transfer properties into one single easily measurable coefficient that is related to the permeability [27]. Thus, at the coating shell surface, we use the more general interlayer conditions Eq. (2.10) rather than Eq. (2.6). Note that Eq. (2.10) includes two limit cases for P (or D_m): when $P = 0$ the case of impermeable coating ($\nabla c_n = 0$) is obtained, and if $P \to \infty$ (coating in perfect contact) the case $c_n = \sigma_n c_s$, similar to the other interlayer conditions (cfr. eqn. (2.6)), is recouped.

3. A case study: the spherical core-shell capsule

The two-layer capsule is currently the most used in the applications and here we consider this special case: a drug-filled core Ω_0 encapsulated by a single polymeric shell Ω_1 and surrounded by the release medium Ω_2: each medium has the shape of concentric sphere of increasing radius, R_0, R_1, R_∞ respectively (with $R_0 < R_1 \ll R_\infty$). This method can be easily extended, with a more complicated algebra, to any number of layers. Due to the homogeneity and isotropy, we can assume that net drug diffusion occurs along the radial direction only, and thus we restrict our study to a one-dimensional model (Fig. 2) that reflects a perfectly radially symmetric system. Thus, the general formulation given in Section 2 reduces to a three coupled equations problem, that in 1D radial symmetry reads:

$$\frac{\partial c_0}{\partial t} = D_0\left(\frac{\partial^2 c_0}{\partial r^2} + \frac{2}{r}\frac{\partial c_0}{\partial r}\right) = \frac{D_0}{r^2}\frac{\partial}{\partial r}\left(r^2 \frac{\partial c_0}{\partial r}\right) \quad \text{in } (0, R_0) \tag{3.1}$$

$$\frac{\partial c_1}{\partial t} = D_1\left(\frac{\partial^2 c_1}{\partial r^2} + \frac{2}{r}\frac{\partial c_1}{\partial r}\right) = \frac{D_1}{r^2}\frac{\partial}{\partial r}\left(r^2 \frac{\partial c_1}{\partial r}\right) \quad \text{in } (R_0, R_1) \tag{3.2}$$

$$\frac{\partial c_2}{\partial t} = D_2\left(\frac{\partial^2 c_2}{\partial r^2} + \frac{2}{r}\frac{\partial c_2}{\partial r}\right) = \frac{D_2}{r^2}\frac{\partial}{\partial r}\left(r^2 \frac{\partial c_2}{\partial r}\right) \quad \text{in } (R_1, R_\infty) \tag{3.3}$$

$$\frac{\partial c_0}{\partial r} = 0 \quad \text{at } r = 0 \tag{3.4}$$

$$-D_0 \frac{\partial c_0}{\partial r} = -D_1 \frac{\partial c_1}{\partial r}, \quad c_0 = \sigma_0 c_1 \quad \text{at } r = R_0 \tag{3.5}$$

$$-D_1 \frac{\partial c_1}{\partial r} = -D_2 \frac{\partial c_2}{\partial r} = P(c_1 - \Sigma c_2) \quad \text{at } r = R_1 \tag{3.6}$$

$$c_2 = 0 \quad \text{at } r = R_\infty \tag{3.7}$$

where r is the radial coordinate position. The initial condition for a releasing capsule is:

$$\begin{aligned} c_0(r,0) &= C_0 \quad \text{for} \quad 0 < r \le R_0 \\ c_1(r,0) &= 0 \quad \text{for} \quad R_0 < r \le R_1 \\ c_2(r,0) &= 0 \quad \text{for} \quad R_1 < r \le R_\infty \end{aligned} \tag{3.8}$$

with C_0 is the initial concentration of the loaded drug in the core.

3.1. The release distance R_∞

The release medium is here delimited by a cut-off finite distance R_∞, whose range is determined by the following considerations. Strictly speaking, for a pure diffusion problem from a spherical source into a homogeneous medium having the diffusivity D, the concentration field $c(\cdot, t)$ undergoes a exponential decay $\propto \exp(-Dt)$ and vanishes asymptotically at infinite distance. On the other hand, at a given time, the concentration is gradually damped, going down to zero at infinite distance.

For computational practical purposes, we set a cut-off length R_∞, that we call *release distance* or *diffusion length*, beyond which the concentration as well as the mass flux reduce to zero, within a prescribed tolerance, at a given time. More precisely, the *release distance* at time t is the minimum finite length such that: $c(R_\infty, t) = \varepsilon c_0 \simeq 0$, with ε a small number. For $0 \le r \le R_\infty$ the concentration decays with time at exponential rate and the sink condition (3.7) holds at R_∞ within the tolerance ε, being $c(r, t) \simeq 0$ for $r \ge R_\infty$. Analogously to the heat transfer problem, R_∞ is proportional to $\sqrt{Dt}$ [28]. The precise estimation of the release distance in a multi-layer medium is beyond the scope of this work, even though there are attempts to compute it within a certain degree of accuracy. However, by considering a homogeneous medium at constant concentration faced with the release medium, we get a conservative overestimation of the release distance by $R_\infty = \sqrt{10mDt}$, with $\varepsilon = 10^{-m}$ [23].

3.2. Solving procedure

We use the separation of variables method to solve the three-layer equation model, as done in other composite release systems [23,24]. To this purpose, it would be convenient to recast the above equations in a dimensionless form.

3.2.1. Scaling

All the variables, the parameters and the equations are normalized by means of the change of variables:

$$r \to \frac{r}{R_\infty} \qquad t \to \frac{D_{max}}{R_\infty^2} t \qquad c_i \to \frac{c_i}{C_0} \tag{3.9}$$

and by introducing the nondimensional constants:

$$R_{0/1/\infty} = \frac{R_{0/1/\infty}}{R_\infty} \qquad \gamma_i = \frac{D_i}{D_{max}} \qquad \phi = \frac{PR_\infty}{D_{max}} \tag{3.10}$$

where subscript max denotes the maximum value across the 3 layers. By separating $c_i(r, t) = F_i(r)G_i(t)$, Eqs. (3.1)–(3.3) become:

$$\frac{1}{\gamma_i}\frac{G_i'}{G_i}=\frac{\left(r^2F_i'\right)'}{r^2F_i}=-\lambda_i^2 \quad i=0,1,2 \tag{3.11}$$

that admits the solutions:

$$F_i(r)=a_i\frac{\cos(\lambda_i r)}{r}+b_i\frac{\sin(\lambda_i r)}{r},\quad G_i(t)=\exp\left(-\gamma_i\lambda_i^2 t\right)\quad i=0,1,2 \tag{3.12}$$

In order to retain a finite solution in $r=0$, we set $a_0=0$. By imposing $G_0=G_1=G_2$ [23], we obtain

$$\lambda_i=\sqrt{\frac{\gamma_0}{\gamma_i}}\lambda_0 \quad i=1,2 \tag{3.13}$$

The boundary condition (3.4) is automatically satisfied, whereas (3.5)–(3.7) read respectively:

$$\gamma_0F_0'(R_0)=\gamma_1F_1'(R_0) \tag{3.14}$$

$$F_0(R_0)=\sigma_0F_1(R_0) \tag{3.15}$$

$$\gamma_1F_1'(R_1)=\gamma_2F_2'(R_1) \tag{3.16}$$

$$\gamma_1F_1'(R_1)+\phi(F_1(R_1)-\Sigma F_2(R_1))=0 \tag{3.17}$$

$$F_2(1)=0 \tag{3.18}$$

This set of 5 algebraic equations (3.14)–(3.18) is made explicit as:

$$\begin{cases}
\gamma_0[R_0\lambda_0\cos(\lambda_0R_0)-\sin(\lambda_0R_0)]b_0+\gamma_1[R_0\lambda_1\sin(\lambda_1R_0)+\cos(\lambda_1R_0)]a_1\\
-\gamma_1[R_0\lambda_1\cos(\lambda_1R_0)-\sin(\lambda_1R_0)]b_1=0\\
\\
\sin(\lambda_0R_0)b_0-\sigma_0\cos(\lambda_1R_0)a_1-\sigma_0\sin(\lambda_1R_0)b_1=0\\
\\
-\gamma_1[R_1\lambda_1\sin(\lambda_1R_1)+\cos(\lambda_1R_1)]a_1+\gamma_1[R_1\lambda_1\cos(\lambda_1R_1)-\sin(\lambda_1R_1)]b_1\\
+\gamma_2[R_1\lambda_2\sin(\lambda_2R_1)+\cos(\lambda_2R_1)]a_2-\gamma_2[R_1\lambda_2\cos(\lambda_2R_1)-\sin(\lambda_2R_1)]b_2=0\\
\\
[-\gamma_1R_1\lambda_1\sin(\lambda_1R_1)+(\phi R_1-\gamma_1)\cos(\lambda_1R_1)]a_1\\
[+\gamma_1R_1\lambda_1\cos(\lambda_1R_1)+(\phi R_1-\gamma_1)\sin(\lambda_1R_1)]b_1\\
-\phi\Sigma R_1\cos(\lambda_2R_1)a_2-\phi\Sigma R_1\sin(\lambda_2R_1)b_2=0\\
\\
\cos(\lambda_2)a_2+\sin(\lambda_2)b_2=0
\end{cases}$$

and form a homogeneous system with unknowns b_0,a_1,b_1,a_2,b_2. By imposing the coefficient matrix to be singular and by using Eq. (3.13), we get a relationship in λ_0 (eigencondition). This problem is solved numerically with MATLAB by a successive bisection method [29]. It admits an infinite number of roots (λ_0^k) with $k=1,2,\ldots$, and from them, the whole set of eigenvalues (λ_i^k) with $i=1,2$ and $k=1,2,\ldots$ are determined. From each eigenvalue, the constants a_i^k,b_i^k are obtained subsequently from Eqs. (3.14)–(3.18), and the eigenfunctions defined in Eq. (3.12) have the form:

$$F_{ik}(r)=a_i^k\frac{\cos\left(\lambda_i^kr\right)}{r}+b_i^k\frac{\sin\left(\lambda_i^kr\right)}{r},\quad k=1,2,\ldots \tag{3.19}$$

4. Computing drug concentration and mass

Once the eigenvalues λ_0^k are computed, the corresponding time-variable functions G_i^k defined by Eq. (3.12) are obtained as:

$$G_0^k(t)=G_1^k(t)=G_2^k(t)=\exp\left(-\gamma_0\left(\lambda_0^k\right)^2t\right) \tag{4.1}$$

Thus, the general solution of the problem (3.1)–(3.8) is given by a linear superposition of the fundamental solutions (3.19)–(4.1) in the form:

$$c_i(r,t)=\sum_{k=1}^{\infty}A_kF_{ik}(r)\exp\left(-\gamma_i\left(\lambda_i^k\right)^2t\right)\quad i=0,1,2 \tag{4.2}$$

where the Fourier coefficients A_k are computed in accordance with the initial conditions:

$$\begin{array}{lll}
c_0(r,0)=1 & \text{for} & 0<r\le R_0\\
c_1(r,0)=0 & \text{for} & R_0<r\le R_1\\
c_2(r,0)=0 & \text{for} & R_1<r\le 1
\end{array} \tag{4.3}$$

By evaluating Eq. (4.2) at $t=0$ and multiplying it by r^2F_{ip}, after integration we get:

$$\int_0^{R_0}\sum_kA_kr^2F_{0k}F_{0p}\,dr=\int_0^{R_0}r^2F_{0p}\,dr \tag{4.4}$$

$$\int_{R_0}^{R_1}\sum_kA_kr^2F_{1k}F_{1p}\,dr=0 \tag{4.5}$$

$$\int_{R_1}^{1}\sum_kA_kr^2F_{2k}F_{2p}\,dr=0 \tag{4.6}$$

By summing (4.4) with (4.5) multiplied by σ_0 and with (4.6) multiplied by $\sigma_0\sigma_1$, and by the orthogonality of F_{0k},F_{1k},F_{2k} (see appendix), we have:

$$A_p\left(\int_0^{R_0}r^2F_{0p}^2dr+\sigma_0\int_{R_0}^{R_1}r^2F_{1p}^2dr+\sigma_0\sigma_1\int_{R_1}^{1}r^2F_{2p}^2dr\right)=\int_0^{R_0}r^2F_{0p}dr \tag{4.7}$$

By setting:

$$I_p=\int_0^{R_0}\sin(\lambda_0^pr)rdr=\left[\frac{\sin(\lambda_0^pr)}{(\lambda_0^p)^2}-\frac{r\cos(\lambda_0^pr)}{\lambda_0^p}\right]_0^{R_0}=\frac{\sin(\lambda_0^pR_0)}{(\lambda_0^p)^2}-\frac{R_0\cos(\lambda_0^pR_0)}{\lambda_0^p} \tag{4.8}$$

we have:

$$A_p=\frac{b_0^pI_p}{N_p} \tag{4.9}$$

with N_p is the norm (see appendix). The analytic form of the solution allows an easy computation of the dimensionless drug mass in each layer as a function of time:

$$\begin{aligned}
M_0(t)&=\int_0^{2\pi}d\phi\int_0^{\pi}\sin\theta\,d\theta\int_0^{R_0}r^2\,c_0(r,t)\,dr=4\pi\int_0^{R_0}r^2\,c_0(r,t)\,dr\\
M_1(t)&=4\pi\int_{R_0}^{R_1}r^2\,c_1(r,t)\,dr\\
M_2(t)&=4\pi\int_{R_1}^{1}r^2\,c_2(r,t)\,dr
\end{aligned} \tag{4.10}$$

In particular, the above Eqs., together with (4.2), yield:

$$M_0(0)=\frac{4}{3}\pi R_0^3,\qquad M_1(0)=M_2(0)=0 \tag{4.11}$$

Moreover, it is easy to verify that $\lim_{t\to\infty}M_0(t)=\lim_{t\to\infty}M_1(t)=0$ and $\lim_{t\to\infty}M_2(t)=M_0(0)$. By Eq. (4.2), we get an explicit computation of M_0,M_1,M_2:

$$\begin{aligned}
M_0(t)=4\pi\sum_kA_k\exp\left(-\gamma_0\left(\lambda_0^k\right)^2t\right)\int_0^{R_0}F_{k0}(r)\,r^2dr=4\pi\sum_kA_k\exp\left(-\gamma_0\left(\lambda_0^k\right)^2t\right)\\
\times\left\{a_0^k\left[\frac{\cos\left(\lambda_0^kR_0\right)}{\left(\lambda_0^k\right)^2}+\frac{R_0\sin\left(\lambda_0^kR_0\right)-1}{\lambda_0^k}\right]+b_0^k\left[\frac{\sin\left(\lambda_0^kR_0\right)}{\left(\lambda_0^k\right)^2}-\frac{R_0\cos\left(\lambda_0^kR_0\right)}{\lambda_0^k}\right]\right\}
\end{aligned} \tag{4.12}$$

$$M_1(t) = 4\pi\sum_k A_k \exp\left(-\gamma_1\left(\lambda_1^k\right)^2 t\right)\int_{R_0}^{R_1} F_{k1}(r)\, r^2 dr = 4\pi\sum_k A_k \exp\left(-\gamma_1\left(\lambda_1^k\right)^2 t\right)$$
$$\times\left\{a_1^k\left[\frac{\cos\left(\lambda_1^k R_1\right)-\cos\left(\lambda_1^k R_0\right)}{\left(\lambda_1^k\right)^2}+\frac{R_1\sin\left(\lambda_1^k R_1\right)-R_0\sin\left(\lambda_1^k R_0\right)}{\lambda_1^k}\right]+b_1^k\left[\frac{\sin\left(\lambda_1^k R_1\right)-\sin\left(\lambda_1^k R_0\right)}{\left(\lambda_1^k\right)^2}-\frac{R_1\cos\left(\lambda_1^k R_1\right)-R_0\cos\left(\lambda_1^k R_0\right)}{\lambda_1^k}\right]\right\} \tag{4.13}$$

$$M_2(t) = 4\pi\sum_k A_k \exp\left(-\gamma_2\left(\lambda_2^k\right)^2 t\right)\int_{R_1}^{1} F_{k2}(r)\, r^2 dr = 4\pi\sum_k A_k \exp\left(-\gamma_2\left(\lambda_2^k\right)^2 t\right)$$
$$\times\left\{a_2^k\left[\frac{\cos\left(\lambda_2^k\right)-\cos\left(\lambda_2^k R_1\right)}{\left(\lambda_2^k\right)^2}+\frac{\sin\left(\lambda_2^k\right)-R_1\sin\left(\lambda_2^k R_1\right)}{\lambda_2^k}\right]+b_2^k\left[\frac{\sin\left(\lambda_2^k\right)-\sin\left(\lambda_2^k R_1\right)}{\left(\lambda_2^k\right)^2}-\frac{\cos\left(\lambda_2^k\right)-R_1\cos\left(\lambda_2^k R_1\right)}{\lambda_2^k}\right]\right\} \tag{4.14}$$

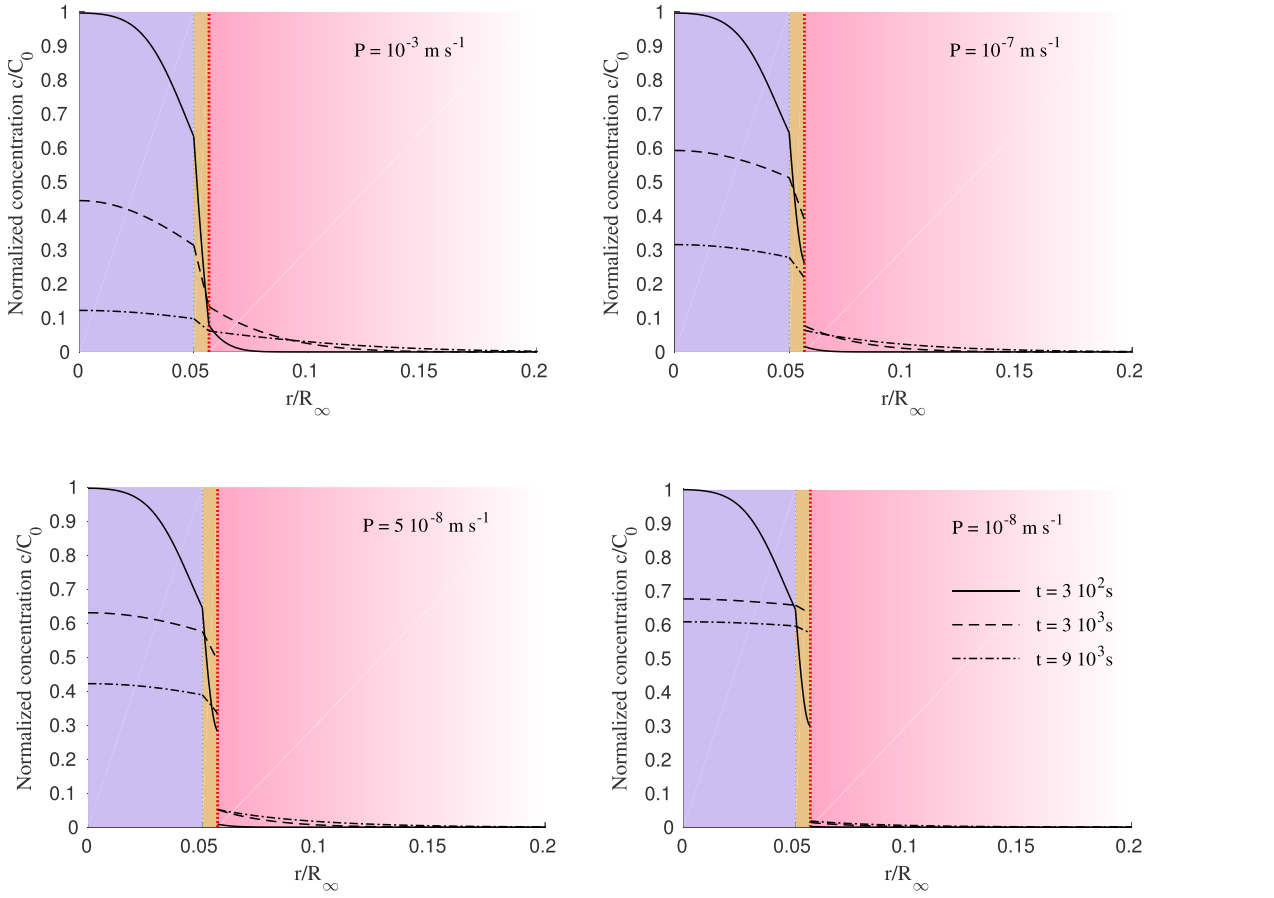

Fig. 3. Normalized radial concentration profiles in the capsule layers (core (*violet*), shell (*yellow*), release medium (*fading pink*)) at three instants, at four values of *P*. At all observable times, all concentrations are damped out at nondimensional distance $r = 0.2$. The core depletion and the drug release slow down at lower *P*. (For interpretation of the references to colour in this figure legend, the reader is referred to the Web version of this article.)

5. Results and discussion

The physical problem of drug release from a multi-layer capsule depends on a large number of parameters. In this article, for simplicity, the following physical parameters are chosen to simulate the release from a coated core-shell drug-loaded capsule. These typical values of geometrical and diffusion parameters are taken from the work of Henning et al. [17]:

$$\begin{array}{lll} R_0 = 1.5{\cdot}10^{-3}m & R_1 = 1.7{\cdot}10^{-3}m & \sigma_0 = \sigma_1 = 1 \\ D_0 = 30{\cdot}10^{-11}m^2s^{-1} & D_1 = 5{\cdot}10^{-11}m^2s^{-1} & D_2 = 30{\cdot}10^{-11}m^2s^{-1} \end{array} \tag{5.1}$$

while the surface mass transfer coefficient P is varied in an appropriate range and $\Sigma = 1$ (see eqn. (2.10)). For these input numerical values, the release distance $R_\infty = 30{\cdot}10^{-3}m \approx 18R_1$ is estimated to yield a complete drug depletion of the core and a fully release time of about 12 h. All the series appearing in the solution (see Eq. (4.2) and what follow) have been truncated at a finite number of terms $N = 300$ for all times reported in the simulation. A number of grid nodes proportional to the thickness of

Table 1
Percentage of the drug mass α retained in each layer at different times for three coatings of different permeability: A) $P = 10^{-8}$, B) $P = 10^{-7}$, C) $P = 10^{-3}$ ($cm\ s^{-1}$) (max error of 1%). Red values indicate the peak mass values in the hydrogel layer. The reported differences evidence a strong influence of P on the depletion time and delivery characteristics.

time ($s(\simeq h:m)$)	$\alpha_0(\%)$ $A-B-C$	$\alpha_1(\%)$ $A-B-C$	$\alpha_2(\%)$ $A-B-C$
$100\ (\simeq 2m)$	$89-89-89$	$11-11-11$	$0-0.03-0.4$
$500\ (\simeq 8m)$	$77-77-75$	$23-22-15$	$0.05-2.3-10$
$10^3\ (\simeq 17m)$	$72-70-64$	$28-24-14$	$0.7-7.1-22$
$3\cdot 10^3\ (50m)$	$67-55-37$	$30-21-10$	$3.9-25-54$
$6\cdot 10^3\ (1h:40m)$	$64-40-19$	$28-15-5.8$	$8.7-46-76$
$10^4\ (\simeq 2h:47m)$	$60-27-9.2$	$26-10-3.1$	$14-64-89$
$3\cdot 10^4\ (\simeq 8h:20m)$	$43-4.8-1.4$	$19-1.9-0.6$	$39-94-99$
$4.32\cdot 10^4\ (12h)$	$35-1.9-0.7$	$15-0.8-0.3$	$51-98-100$

the layer to guarantee a convenient resolution has been considered. For example, for the layer's sizes corresponding to the above parameters, a number of equidistributed 100, 14 and 1888 points has been selected, respectively.

Drug is transported differently in each layer, that receives mass from the underneath layer and transmits it to the next above, in a cascade sequence until the drug is completely released at finite distance R_∞ for a sufficiently long time. The effect of the combined multi-layer diffusivity is similar to that of other releasing systems [23]. Here we analyze the behavior of the profile at varying mass transfer coefficient P. Fig. 3 shows the concentration profiles in the case of different coated capsules, and reports a different release in the various configurations ranging from a fully permeable (Fig. 3 top left) to the almost impermeable case (Fig. 3 bottom right). It turns out that for the above parameters, the sensitive values are in the range: $10^{-8} \le P \le 10^{-3}$. For $P < 10^{-8}$, the coating acts as an impermeable barrier *(as $P\to 0$)*, for $P > 10^{-3}$, the capsule surface results in perfect contact with the surrounding external medium *(as $P\to\infty, \Sigma = 1$)*, giving rise to the concentration continuity.

Concentration is dropping down inside each layer, being possibly discontinuous at the interlayer interfaces, with the mass flux continuity preserved (Fig. 3). We also compute the fraction of drug mass retained in each layer, defined as:

$$\alpha_i(t) = \frac{M_i(t)}{M_0(0)} \quad i = 0, 1, 2 \tag{5.2}$$

Table 1 gives the different distribution of $\alpha_i(t)$ in each layer, in three significant cases of coating having different permeability. Because of the sink boundary condition (3.7), all mass eventually accumulates in the external release medium up to a distance R_∞. In other words, due to the absorbing condition (3.7) at the release distance, all drug mass is transferred to the external medium at a sufficiently long time and the total mass is preserved and equals its initial value (say the drug mass in the coating $M_0(0)$*)*, such that:

$$\frac{M_0(0) - \sum_{i=0}^{2} M_i(t)}{M_0(0)} = 1 - \sum_{i=0}^{2} \alpha_i(t) \simeq 0 \tag{5.3}$$

The drug mass is monotonically decreasing in the core (layer 0), but is first increasing up to some upper bound and then decaying asymptotically in the layer 1 (Fig. 4). In the release medium the mass progressively accumulates over an extended distance R_∞ at a time depending on the

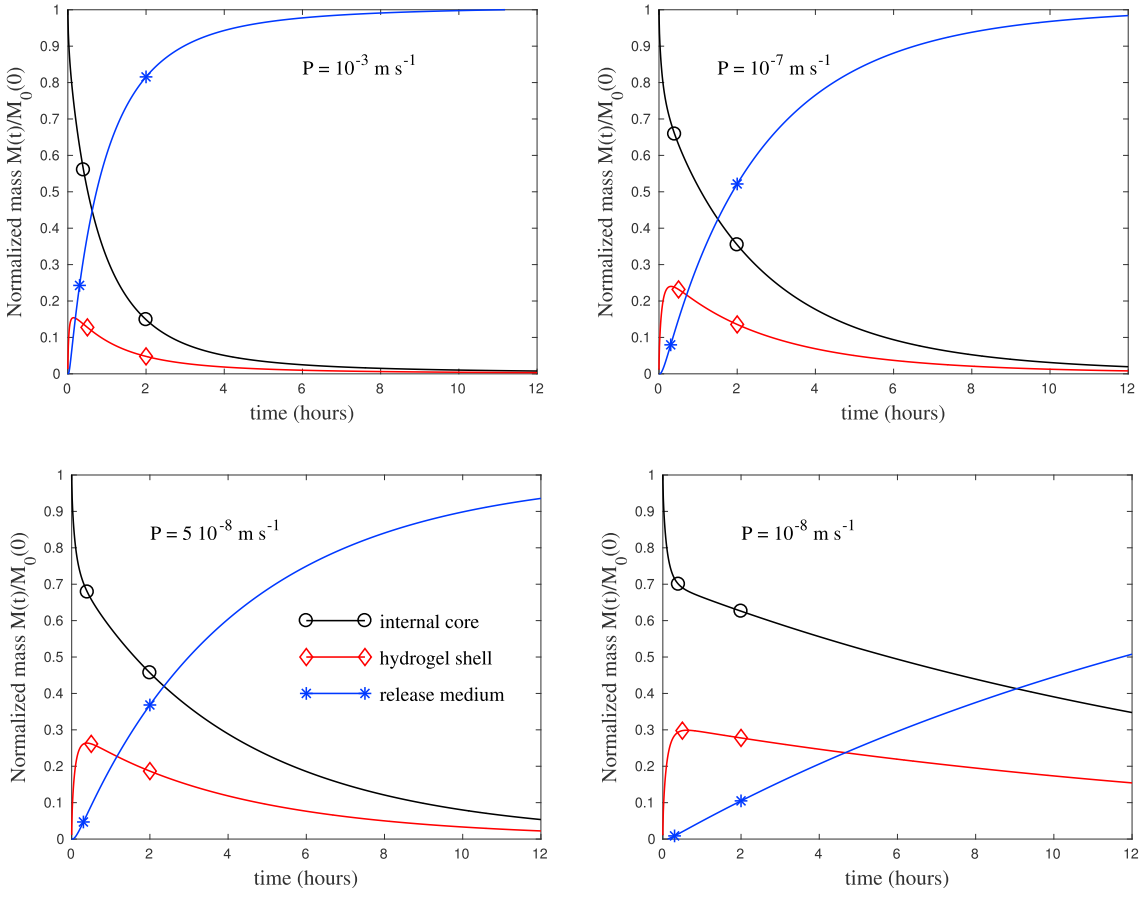

Fig. 4. Normalized drug mass profiles in the internal core (layer 0), in the hydrogel shell (layer 1) and in the targeted release medium (layer 2) at four values of P. In the innermost layer mass is monotonically decreasing, in the release medium the profile is raising up to a complete release, while in the hydrogel there is a characteristic time at which the drug reaches a peak. Note a more uniform and sustained release at lower P.

diffusive properties of the two-layer capsule. The simulation points out the time and the size of the mass peak in the hydrogel layer (layer 1) is related to the releasing properties of the core at one hand, and to the diffusivity of the release medium at the other hand, together with the mass resistance of the coating. The thin hydrogel layer retains a negligible mass due to its thickness, and the core is completely emptied after a period of about 12 h (Table 1) in the case of $P \geq 10^{-3}$. At that time, all the mass is transferred to the external layer. A much sustained release occurs in the case of a coating having a smaller mass transfer coefficient ($P \leq 10^{-7}$).

It appears also that the relative size of the layers and their respective diffusivity affect the whole drug release processes. Thus, depending on the specific application, it is worth identifying which set of parameters guarantees a more prolonged and uniform release and what other values are responsible for a localized peaked distribution followed by a faster decay. One of them is the permeability of the coating shell that offers a significant resistance to the mass flux. Thus, the coating resistance has to be properly tuned in order to allow drug molecules to be released, while maintained in the efficient therapeutic range without exceeding the toxic dose nor dropping below an insufficient dose. These results can be used to assess whether drug targets tissues at the desired rate and to optimize the dose capacity given by thin surface coating shells for an extended period of time. Differently than in other single layer models, the current formulation constitutes a simple tool to predict the accurate drug release from a multi-layer coated capsule that can help in designing and in manufacturing new drug delivery platforms.

6. Conclusions

Despite notable recent progress in designing drug release systems, the precise characteristics and the development of multifunctional delivery carriers remains a challenge. Mathematical modelling has emerged in recent years as an additional powerful alternative tool to simulate drug delivery processes and much effort is currently addressed for a deeper understanding of the elution mechanism. This is not completely understood and can be influenced by different concurrent physical and chemical factors. In this work we propose a mechanistic model for studying the drug release from a multi-layer coated spherical capsule under a limited number of physical assumptions. The analytic form of the solution provides insights into the drug mass transfer as well as the effect of parameters, such as the device geometry and the coating resistance, on the release mechanism. By showing the relationship among the several variables and material transport properties, the present model can be used to identify and optimize parameters to guarantee a controlled delivery. Thus, the capsule design for a therapeutically optimal rate can be predicted using a systematic approach with a minimum number of experimental studies.

Acknowledgments

We are grateful to E.J. Carr of the Queensland University of Technology, F. de Monte of the University of L'Aquila and R. Jellali of the University of Technology of Compiègne for their valuable discussions and helpful comments. This work was partially supported by the Région Hauts de France through the CapsAntiOx project (RDIPROJINV-000086, RDIPROJFT-000198). We kindly acknowledge support by a STSM Grant from EU COST Action 15120 Open Multiscale Systems Medicine (OpenMultiMed).

Appendix

Let us prove the orthogonality of the system $F_{ik}(r),\ i = 0, 1, 2, \quad k = 1, 2, \ldots.$ – see Eq. (3.19) – in the interval $[0, 1]$. The Sturm-Liouville eigenvalue problems Eq. (3.11) can be written:

$$\left(r^2 F_0^{'}\right)^{'} = -\lambda_0^2 r^2 F_0 \quad \text{in } [0, R_0] \tag{A.1}$$

$$F_0'(0) = 0 \tag{A.2}$$

$$\gamma_0 F_0'(R_0) = \gamma_1 F_1'(R_0) \tag{A.3}$$

$$\left(r^2 F_1^{'}\right)^{'} = -\lambda_1^2 r^2 F_1 \quad \text{in } [R_0, R_1] \tag{A.4}$$

$$F_0(R_0) = \sigma_0 F_1(R_0) \tag{A.5}$$

$$\gamma_1 F_1'(R_1) = \gamma_2 F_2'(R_1) \tag{A.6}$$

$$\left(r^2 F_2^{'}\right)^{'} = -\lambda_2^2 r^2 F_2 \quad \text{in } [R_1, 1] \tag{A.7}$$

$$F_1(R_1) = \sigma_1 F_2(R_1) \tag{A.8}$$

$$F_2(1) = 0 \tag{A.9}$$

Let us consider two different eigenvalues λ_{0m} and λ_{0n} and the corresponding eigenfunctions F_{0m}, F_{0n}. Multiplying Eq. (A.1) by F_{0n} and integrating:

$$\lambda_{0m}^2 \int_0^{R_0} r^2 F_{0m} F_{0n} dr = -\int_0^{R_0} \left(r^2 F_{0m}^{'}\right)^{'} F_{0n} dr = -\left[r^2 F_{0m}^{'} F_{0n}\right]_0^{R_0} + \int_0^{R_0} r^2 F_{0m}^{'} F_{0m}^{'} dr \tag{A.10}$$

Similarly, for the eigenvalue λ_{0n}

$$\lambda_{0n}^2 \int_0^{R_0} r^2 F_{0n} F_{0m} dr = -\int_0^{R_0} \left(r^2 F'_{0n}\right)' F_{0m} dr = -\left[r^2 F'_{0n} F_{0m}\right]_0^{R_0} + \int_0^{R_0} r^2 F'_{0n} F'_{0m} dr \tag{A.11}$$

Subtracting Eq. (A.11) from Eq. (A.10) we have:

$$\left(\lambda_{0m}^2 - \lambda_{0n}^2\right) \int_0^{R_0} r^2 F_{0n} F_{0m} dr = -\left[r^2 F_{0m}{}' F_{0n}\right]_0^{R_0} + \left[r^2 F'_{0n} F_{0m}\right]_0^{R_0} \tag{A.12}$$

Repeating a similar procedure for Eq. (A.4) (resp. Eq. (A.7)), for the eigenvalues $\lambda_{1m}, \lambda_{1n}$ (resp. $\lambda_{2m}, \lambda_{2n}$) and for the eigenfunctions F_{1m}, F_{1n} (resp. F_{2m}, F_{2n}), we get:

$$\left(\lambda_{1m}^2 - \lambda_{1n}^2\right) \int_{R_0}^{R_1} r^2 F_{1n} F_{1m} dr = -\left[r^2 F'_{1m} F_{1n}\right]_{R_0}^{R_1} + \left[r^2 F'_{1n} F_{1m}\right]_{R_0}^{R_1} \tag{A.13}$$

$$\left(\lambda_{2m}^2 - \lambda_{2n}^2\right) \int_{R_1}^{1} r^2 F_{2n} F_{2m} dr = -\left[r^2 F'_{2m} F_{2n}\right]_{R_1}^{1} + \left[r^2 F'_{2n} F_{2m}\right]_{R_1}^{1} \tag{A.14}$$

Eq. (A.12) multiplied by γ_0 and by use of (A.2) reads:

$$\gamma_0 \left(\lambda_{0m}^2 - \lambda_{0n}^2\right) \int_0^{R_0} r^2 F_{0n} F_{0m} dr = -\gamma_0 R_0^2 F'_{0m}(R_0) F_{0n}(R_0) + \gamma_0 R_0^2 F'_{0n}(R_0) F_{0m}(R_0) \tag{A.15}$$

Eq. (A.13) multiplied by $\gamma_1 \sigma_0$ gives:

$$\gamma_1 \left(\lambda_{1m}^2 - \lambda_{1n}^2\right) \sigma_0 \int_{R_0}^{R_1} r^2 F_{1n} F_{1m} dr = -\gamma_1 R_1^2 \sigma_0 F'_{1m}(R_1) F_{1n}(R_1) + \gamma_1 R_0^2 \sigma_0 F'_{1m}(R_0) F_{1n}(R_0) + \gamma_1 R_1^2 \sigma_0 F'_{1n}(R_1) F_{1m}(R_1) - \gamma_1 R_0^2 \sigma_0 F'_{1n}(R_0) F_{1m}(R_0) \tag{A.16}$$

Finally Eq. (A.14) multiplied by $\gamma_2 \sigma_0 \sigma_1$ and by use of (A.9) becomes:

$$\gamma_2 \left(\lambda_{2m}^2 - \lambda_{2n}^2\right) \sigma_0 \sigma_1 \int_{R_1}^{1} r^2 F_{2n} F_{2m} dr = \gamma_2 R_1^2 \sigma_0 \sigma_1 F'_{2m}(R_1) F_{2n}(R_1) - \gamma_2 R_1^2 \sigma_0 \sigma_1 F'_{2n}(R_1) F_{2m}(R_1) \tag{A.17}$$

By summing Eqs. (A.15), (A.16), (A.17) and by use of Eqs. (3.13), (A.3) and (A.6) we get:

$$\gamma_0 \left(\lambda_{0m}^2 - \lambda_{0n}^2\right) \left(\int_0^{R_0} r^2 F_{0n} F_{0m} dr + \sigma_0 \int_{R_0}^{R_1} r^2 F_{1n} F_{1m} dr + \sigma_0 \sigma_1 \int_{R_1}^{1} r^2 F_{2n} F_{2m} dr \right) = \gamma_0 R_0^2 F'_{0n}(R_0) [F_{0m}(R_0) - \sigma_0 F_{1m}(R_0)] - \gamma_0 R_0^2 F'_{0m}(R_0) [F_{0n}(R_0) - \sigma_0 F_{1n}(R_0)]$$
$$+ \gamma_1 R_1^2 \sigma_0 F'_{1n}(R_1) [F_{1m}(R_1) - \sigma_1 F_{2m}(R_1)] - \gamma_1 R_1^2 \sigma_0 F'_{1m}(R_1) [F_{1n}(R_1) - \sigma_1 F_{2n}(R_1)] \tag{A.18}$$

Finally, by the use of (A.5) and (A.8), all terms at r.h.s. are zero and

$$\int_0^{R_0} r^2 F_{0n} F_{0m} dr + \sigma_0 \int_{R_0}^{R_1} r^2 F_{1n} F_{1m} dr + \sigma_0 \sigma_1 \int_{R_1}^{1} r^2 F_{2n} F_{2m} dr = \begin{cases} 0 & \text{for} \quad m \neq n \\ N_m & \text{for} \quad m = n \end{cases} \tag{A.19}$$

with

$$N_m = \int_0^{R_0} \left(b_0^m \sin\left(\lambda_0^m r\right)\right)^2 dr + \sigma_0 \int_{R_0}^{R_1} \left(a_1^m \cos\left(\lambda_1^m r\right) + b_1^m \sin\left(\lambda_1^m r\right)\right)^2 dr + \sigma_0 \sigma_1 \int_{R_1}^{1} \left(a_2^m \cos\left(\lambda_2^m r\right) + b_2^m \sin\left(\lambda_2^m r\right)\right)^2 dr > 0 \tag{A.20}$$

the norm.

References

[1] J. Siepmann, R.A. Siegel, J. Rathbone, Fundamental and Applications of Controlled Release Drug Delivery, Springer, 2012.

[2] S. De Koker, R. Hoogenboom, B.G. De Geest, Polymeric multilayer capsules for drug delivery, Chem. Soc. Rev. 41 (2012) 2867–2884.

[3] A.S. Timin, D.J. Gould, G.B. Sukhorukov, Multi-layer microcapsules: fresh insights and new applications, Expet Opin. Drug Deliv. 14 (5) (2016) 583–587.

[4] M. Hassou, F. Couenne, Y. le Gorrec, M. Tayakout, Modeling and simulation of polymeric nanocapsule formation by emulsion diffusion method, AIChE J. 55 (8) (2009) 2094–2105.

[5] Y.-K. Lin, H.-O. Ho, Investigations on the drug releasing mechanism from an asymmetric membrane-coated capsule with an in situ formed delivery orifice, J. Contr. Release 89 (2003) 57–69.

[6] F. Cuomo, F. Lopez, M. Piludu, M.G. Miguel, B. Lindman, A. Ceglie, Release of small hydrophilic molecules from polyelectrolyte capsules: effect of the wall thickness, J. Colloid Interface Sci. 447 (2015) 211–216.

[7] H. Masoud, A. Alexeev, Controlled release of nanoparticles and macromolecules from responsive microgel capsules, Acs Nano 6 (1) (2012) 212–219.

[8] J. Chen, S. Ratnayaka, A. Alford, V. Kozlovskaya, F. Liu, B. Xue, K. Hoyt, E. Kharlampieva, Theranostic multilayer capsules for ultrasound imaging and guided drug delivery, ACS Nano 11 (2017) 3135–3146.

[9] A. Larranaga, M. Lomora, J.R. Sarasua, C.G. Palivan, A. Pandit, Polymer capsules as micro-/nanoreactors for therapeutic applications: current strategies to control membrane permeability, Prog. Mater. Sci. 90 (2017), 325–257.

[10] K.W. Leong, R. Langer, Polymeric controlled drug delivery, Adv. Drug Deliv. Rev. 1 (1987) 199–233.

[11] J. Siepmann, N.A. Peppas, Modeling of drug release from delivery systems based on hydroxypropyl methylcellulose (HPMC), Adv. Drug Deliv. Rev. 48 (2–3) (2001) 139–157.

[12] N.A. Peppas, B. Narasimhan, Mathematical models in drug delivery: how modeling has shaped the way we design new drug delivery systems, J. Contr. Release 190 (2014) 75–81.

[13] M. Grassi, G. Lamberti, S. Cascone, G. Grassi, Mathematical modeling of simultaneous drug release and in vivo absorption, Int. J. Pharm. 418 (2011) 130–141.

[14] J. Siepmann, F. Siepmann, Modeling of diffusion controlled drug delivery, J. Contr. Release 161 (2) (2012) 351–362.

[15] E. Kaunisto, M. Marucci, P. Borgquist, A. Axelsson, Mechanistic modelling of drug release from polymer-coated and swelling and dissolving polymer matrix systems, Int. J. Pharm. 418 (1) (2011) 54–77.
[16] E. Kaunisto, F. Tajarobi, S. Abrahmsen-Alami, A. Larsson, B. Nilsson, A. Axelsson, Mechanistic modelling of drug release from a polymer matrix using magnetic resonance microimaging, Eur. J. Pharmaceut. Sci. 48 (4–5) (2013) 698–708.
[17] S. Henning, D. Edelhoff, B. Ernst, S. Leick, H. Rehage, D. Suter, Characterizing permeability and stability of microcapsules for controlled drug delivery by dynamic NMR microscopy, J. Magn. Reson. 221 (2012) 11–18.
[18] T. Phaechamud, W. Darunkaisorn, Drug release behavior of polymeric matrix filled in capsule, Saudi Pharmaceut. J. 24 (2016) 627–634.
[19] J. Kilinski Tavares, A.A. Ulson de Souza, J.V. de Oliveira, W.L. Priamo, S.M.A. Guelli Ulson de Souza, Modeling of the controlled release of betacarotene into anhydrous ethanol from microcapsules, OpenNano 1 (2016) 25–35.
[20] J. Crank, The Mathematics of Diffusion, Oxford Univ. Press, 1975.
[21] D.Y. Arifin, L.Y. Lee, C.H. Wang, Mathematical modeling and simulation of drug release from microspheres: implications to drug delivery systems, Adv. Drug Deliv. Rev. 58 (2006) 1274–1325.
[22] B. Kaoui, M. Lauricella, G. Pontrelli, Mathematical modelling of drug release from multi-layer capsules, arXiv (2017). https://arxiv.org/abs/1708.01205v1.
[23] G. Pontrelli, F. de Monte, A multi-layer porous wall model for coronary drug-eluting stents, Int. J. Heat Mass Tran. 53 (2010) 3629–3637.
[24] G. Pontrelli, F. de Monte, A two-phase two-layer model for transdermal drug delivery and percutaneous absorption, Math. Biosci. 257 (2014) 96–103.
[25] S. McGinty, G. Pontrelli, A general model of coupled drug release and tissue absorption for drug delivery devices, J. Contr. Release 217 (2015) 327–336.
[26] B. Kaoui, Flow and mass transfer around a core-shell reservoir, Phys. Rev. E 95 (2017) 063310.
[27] E.L. Cussler, Diffusion: Mass Transfer in Fluid Systems, Cambridge Univ. Press, 1997.
[28] A.F. Mills, Heat and Mass Transfer, CRC Press, 1995.
[29] G. Dahlquist, A. Björck, Numerical Methods in Scientific Computing, vol. 1, SIAM, 2008.